Dear author,

In the stage of preparing your full work for evaluation, after receiving approval of the corresponding abstract, we kindly ask you to follow the next steps:

1. Update your approved abstract (you might want to introduce modifications) and submit it now in a written version according to the abstract template (many abstracts were introduced directly into the websystem). This version of the abstract will compose the *abstracts booklet* to be distributed to the participants when registering;

2. Fill the form in the next page, indicating to which section you would like your work to be directed. This will help organizing the sessions according to the mini-symposia advertised rather than in the areas and subareas present in the websystem. We apologize for this possible confusion. The reason is that we are using the websystem provided by ABCM, which does not allow us to introduce thematic sessions freely.

If any doubts arise, please contact us.

Your presence in MecSol 2017 will help making this a very successful event. We look forward to seeing you in Joinville!

With kind regards,

The Organizing Committee
MecSol 2017

6th International Symposium on Solid Mechanics

Click on the box to select the Mini-Symposia:

☐ Multiaxial and Fretting Fatigue (*Edgar Mamiya* and *Lucival Malcher*);

☐ Composite Materials (*Ricardo de Medeiros*);

☐ Constitutive Models I – Plasticity and Damage (*Lucival Malcher*, *Miguel Vaz Jr.* and *Edgar Mamiya*);

☐ Constitutive Models II – Viscoelastic and Viscoplastic Solids: Models and Applications (*Heraldo Mattos*);

☐ Impact Engineering (*Marcílio Alves*);

☐ Structural Reliability Methods and Reliability-Based Design Optimization (*André Beck*);

☐ Topology Optimization of Multifunctional Materials, Fluids and Structures (*Eduardo Lenz Cardoso* e *Emilio Carlos Nelli Silva*);

☐ Topological Derivatives: Theory and Applications (*André Novotny*);

☐ X-FEM, G-FEM and Meshfree Methods (*Roberto Dalledone Machado* and *Rodrigo Rossi*);

☐ High Order Finite Elements (*Marco Lúcio Bittencourt*);

☐ Nonlinear Analyses (*Eduardo Campello*);

☒ Other section;

MECSOL Joinville 2017

April 26-28, 2017
Joinville, Santa Catarina, Brazil

A Finite Element Method for Modelling Vehicle-Track-Bridge Interaction under Moving Loads

Juliana Pereira Rego Remor
Graduate Program in Civil Engineering
Universidade Tecnológica Federal do Paraná
julianaremor@gmail.com
Fernando Luiz Martinechen Beghetto
Graduate Program in Civil Engineering
Universidade Tecnológica Federal do Paraná
flbeghetto@utfpr.edu.br
João Elias Abdalla Filho
Graduate Program in Civil Engineering
Universidade Tecnológica Federal do Paraná
joaofilho@utfpr.edu.br

...

ABSTRACT

A finite element method is applied to analyze the dynamic responses of railway track and bridge under moving loads. The vehicle is a 9 degree-of-freedom model composed of an association of rigid bodies connected via suspension systems. The dynamic responses of the vehicle are obtained due to the speed and tracks irregularities, which are considered as harmonic sinusoidal functions. After that, the vehicle wheel forces are applied on the railway track-bridge model. The dynamic behavior of the railway track-bridge model is studied integrating the rail, ballast, and bridge. The rails are modeled as an elastic Euler-Bernoulli upper beam and the bridge as an Euler-Bernoulli lower beam. The sleepers and ballast are modeled using Winkler foundation for translation. The Rayleigh method is used to define structural damping. The equations of motion of both systems are integrated using Newmark's method. Ballast influence is analyzed.

Keywords: Railways, Vehicle-Track-Bridge Interaction , Finite Element Analysis, Structural Dynamics

1 INTRODUCTION

The dynamic response of railway bridges subject to moving loads has long been an interesting topic in field of civil engineering. A historical review in this topic can be found in reference [1]. Railway bridges are often composed of short-span isostatic bridges, which have been shown to originate high levels of vibration exceeding the limits for comfort and safety.

Railways with better dynamic performance are essential for safe and stable running of trains. Vehicles with better dynamic performance will reduce their damage to railways in the interactions between vehicles and railways. One effective approach to model the dynamic behavior of railway structures as well as for assessing the riding comfort of passengers is to simulate the dynamic vehicle-track-bridge interaction, which remains an open problem if realistic modeling and if high accuracy levels are to be attained. Computational simulation has been adopted by many researchers in several countries in order to perform a close study on the dynamic characteristics of railway structures to

replace the costly and time-consuming physical tests. Different models have been developed and great progress achieved [13].

This paper describes a finite element model for investigating the interactions among a moving train and a track-bridge system. The moving train is modeled with nine-degrees-of-freedom (9-DOF) vehicle consisting of 8 sprung masses (wheels) and 3 unsprung masses interconnected. The vehicle forces are applied at discrete points of the bridge. The rail is modeled as an upper Euler-Bernoulli beam and the bridge as a lower Euler-Bernoulli beam. The two beams are interconnected by a series of springs and dampers. Three-dimensional models to represent the railway bridge and vehicle are developed, and they are numerically implemented in a MATLAB code. Numerical applications are performed. Mid span displacement is analyzed and compared. The ballast stiffness and damping adopted are obtained from other research works [2]-[13] and displacement results associated to those different values of data are compared.

2 THEORY AND FORMULATION

This section describes the mathematical models adopted for the vehicle, bridge and track irregularities. Also, it describes the model adopted for the interaction of the track and the bridge, which takes into account the ballast effect.

2.1 Vehicle Modeling

Figure 1 illustrates the three-dimensional vehicle model adopted in this study and shows the prestressed concrete bridge longitudinal view and cross-section. The vehicle program model is taken from [14] and implemented in this study.

The vehicle consists of a car body, two bogie frames and four wheel sets. The vehicle model is capable of representing bouncing (Z), rolling (ϕ) and pitching (θ) movements in each rigid body, totalizing nine degrees-of-fredom (9 DOF). These three movements are vertical displacement and rotations around the Y and X axes, respectively, as shown in Figure 1. The model is composed of an association of the rigid bodies connected by suspensions systems. These rigid bodies have homogeneous mass m and moments of inertia I_X and I_Y. The primary suspensions, located between wheels and bogies, are represented by linear springs and dampers with coefficients K_P and C_P, and the secondary suspensions, located between the bogies and the car body, are represented by linear springs and dampers with coefficients K_S and C_S. The vehicle moving with constant speed over the bridge is subject to track irregularities, which produces harmonic sinusoidal displacements δ on the suspensions.

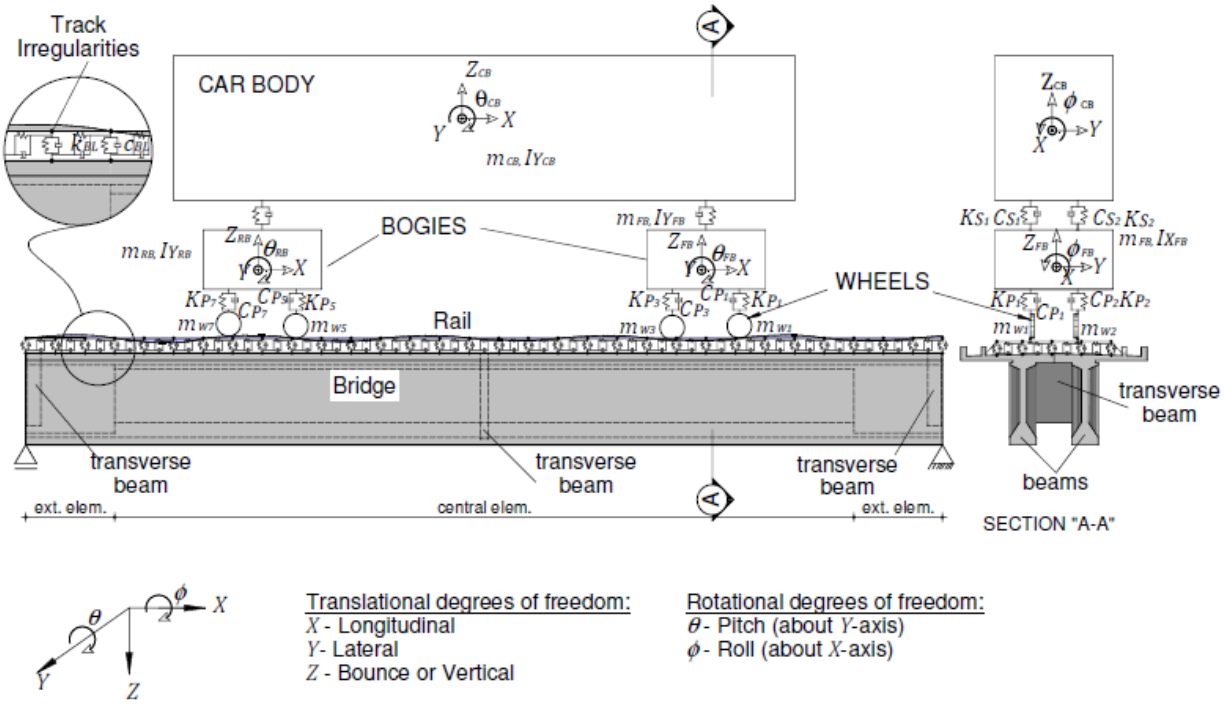

Figure 1: Vehicle model

2.2 Bridge Modeling

The top view of the finite element bridge model is shown in Figure 2. The numbers 1 to 63 are the Euler-Bernoulli elements used in the model, and Pw1 to Pw8 represent the wheel-track contact points, which are the points where the vehicle forces are applied onto the bridge.

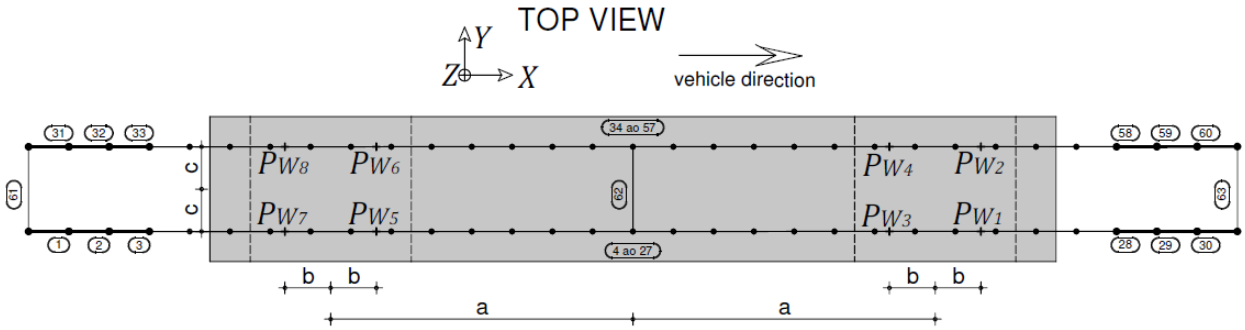

Figure 2: Finite element bridge model top view

Figure 3 shows a lateral view of the model of Figure 2, which represents the interaction between rail, ballast and bridge for each element of the model. A typical track-bridge element is highlighted in the figure. In such element, the rail is represented as an upper beam with 3-DOF per node (U_{Ri},

V_{Ri}, M_{Ri}), the bridge is represented as a lower beam with the same 3-DOF per node (U_{Bi}, V_{Bi}, M_{Bi}), and the ballast between both beam elements is represented springs and dampers of longitudinal and transverse actions.

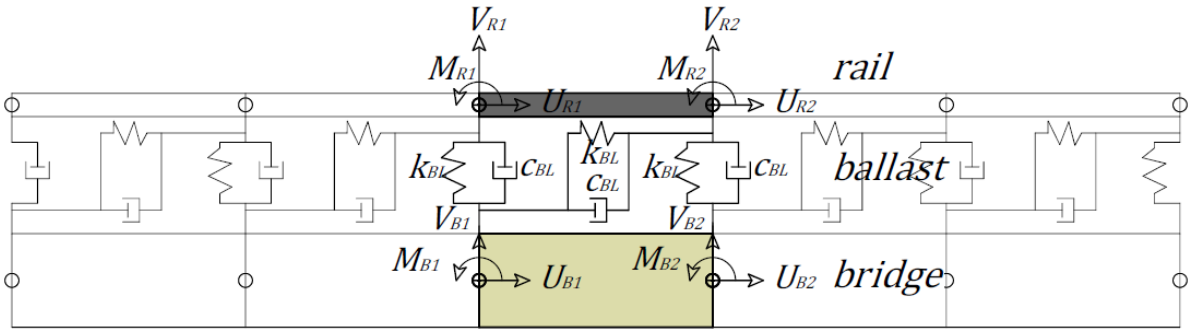

Figure 3: Finite element: track-bridge interaction

2.3 Vehicle Equations

The vehicle equations of motion are obtained using the dynamic equilibrium of the system forces and can be written as:

$$[M_T]\{\ddot{U}\} + [C_T]\{\dot{U}\} + [K_T]\{U\} = \{F_T(t)\} \tag{1}$$

where:

$[M_T]$ denotes the vehicle mass, $[C_T]$ denotes the vehicle viscous damping, $[K_T]$ denotes the vehicle stiffness, and $\{F_T(t)\}$ denotes the vehicle force vector due to rail irregularities. The nine equations of motion are shown explicitly below:

$$\begin{bmatrix} m_{CB} & & & & & & & & & \\ & I_{Y_{CB}} & & & & & & & & \\ & & I_{X_{CB}} & & & & & & & \\ & & & m_{FB} & & & & & & \\ & & & & I_{Y_{FB}} & & & & & \\ & & & & & I_{X_{FB}} & & & & \\ & & & & & & m_{RB} & & & \\ & & & & & & & I_{Y_{RB}} & & \\ & & & & & & & & I_{X_{RB}} & \end{bmatrix} * \begin{Bmatrix} \ddot{Z}_{CB} \\ \ddot{\phi}_{CB} \\ \ddot{\theta}_{CB} \\ \ddot{Z}_{FB} \\ \ddot{\phi}_{FB} \\ \ddot{\theta}_{FB} \\ \ddot{Z}_{RB} \\ \ddot{\phi}_{RB} \\ \ddot{\theta}_{RB} \end{Bmatrix} + \quad [C_T] * \begin{Bmatrix} \dot{Z}_{CB} \\ \dot{\phi}_{CB} \\ \dot{\theta}_{CB} \\ \dot{Z}_{FB} \\ \dot{\phi}_{FB} \\ \dot{\theta}_{FB} \\ \dot{Z}_{RB} \\ \dot{\phi}_{RB} \\ \dot{\theta}_{RB} \end{Bmatrix} + \quad (2)$$

$$[K_T] * \begin{Bmatrix} Z_{CB} \\ \phi_{CB} \\ \theta_{CB} \\ Z_{FB} \\ \phi_{FB} \\ \theta_{FB} \\ Z_{RB} \\ \phi_{RB} \\ \theta_{RB} \end{Bmatrix} = \begin{Bmatrix} 0 \\ 0 \\ 0 \\ \sum_{i=1}^{4} C_{P_i} \dot{I}_R + K_{P_i} I_R \\ \sum_{i=1}^{4} (-1)^i \left(C_{P_i} c \dot{I}_{R_i} + K_{P_i} c I_{R_i} \right) \\ \sum_{i=1}^{2} C_{P_i} b \dot{I}_{R_i} + K_{P_i} b I_{R_i} - \sum_{i=3}^{4} C_t b \dot{I}_{R_i} + K_{P_i} b I_{R_i} \\ \sum_{i=5}^{8} C_{P_i} \dot{I}_{R_i} + K_{P_i} I_{R_i} \\ \sum_{i=5}^{6} (-1)^i \left(C_{P_i} c \dot{I}_{R_i} + K_{P_i} c I_{R_i} \right) \\ \sum_{i=1}^{4} C_{P_i} b \dot{I}_{R_i} + K_{P_i} b I_{R_i} - \sum_{i=5}^{8} C_{P_i} b \dot{I}_{R_i} + K_{P_i} b I_{R_i} \end{Bmatrix}$$

where:

- The symbols $(\cdot)$ and $(\cdot\cdot)$ above the variables, represents the first and the second differentiation with respect of time.
- m_{CB}, m_w and m_B represent the car body mass, wheel and bogie mass, respectively;
- $I_{Y_{CB}}$, $I_{X_{CB}}$, $I_{Y_{FB}}$, $I_{X_{FB}}$, $I_{Y_{RB}}$ and $I_{X_{RB}}$ represent the moment of inertia of the car body, the front bogie and the rear bogie for Y and X direction, respectively;
- Z_{CB}, Z_{FB} and Z_{RB} represent the translations along the Z axis of the car body, the front bogie and the rear bogie, respectively;
- ϕ_{CB}, $\phi_{FB}$and ϕ_{RB} represent the rotation along the X axis of the car body, the front bogie and the rear bogie, respectively;
- θ_{CB}, θ_{FB}, and θ_{RB} represent the rotation along the Y axis of the car body, the front bogie and the back bogie, respectively;
- I_R (t) are the vertical track irregularities indicated in equations (4) and (5).
- K_P and C_P are the linear springs and dampers of the primary suspensions, located between wheels and bogies.

The vehicle forces are transmitted to the bridge structure at the contact points (Pw). These forces are obtained from the contribution of vehicle weight and inertial forces, that is

$$F_{R_i}(t) = \left(\frac{m_{CB}}{8} + \frac{m_B}{4} + m_{W_i} \right) g + m_{w_i} \ddot{I}_{R_i}(t) + c_{P_i} \dot{\delta}_{P_i} + k_{P_i} \delta_{P_i(t)} + \frac{c_{S_i} \dot{\delta}_{S_i}}{2} + \frac{k_{S_i} \delta_{S_i(t)}}{2} \quad (3)$$

where:

- $F_R(t)$ are the forces applied on the bridge from every vehicle wheel;
- m_{CB}, m_w and m_B represents the car body mass, wheel and bogie mass, respectively;
- $\ddot{I}_R(t)$ is the acceleration caused by the track irregularities, that is, the second derivative with respect to time of $I_R(t)$;
- c_P and c_S represent viscous damping of primary and secondary suspensions, respectively;
- k_P and k_S represent stiffness of primary and secondary suspensions, respectively;
- δ_P and δ_S represent displacements at the primary and secondary suspensions, respectively. The symbol $(\cdot)$ above the displacements, represents the first differentiation with respect to time.

2.4 Track Irregularities

The track irregularities I_R are represented by harmonic functions which are described by the equation and figure below:

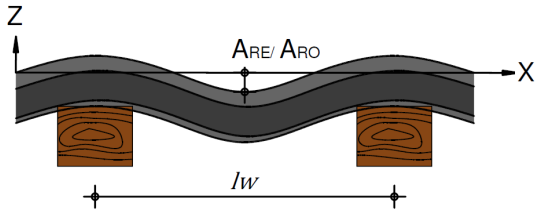

Figure 4: Vertical track irregularities

$$I_{R_{2i}}(t) = A_{RE} sen\left[\frac{2\pi v}{l_W}\left(t + \frac{|P_{W_{2i}} - P_{W_2}|}{v}\right)\right] \qquad for\ i = 1,\ldots,4 \qquad (4)$$

$$I_{R_{2i-1}}(t) = A_{RO} sen\left[\frac{2\pi v}{l_W}\left(t + \frac{|P_{W_{2i-1}} - P_{W_i}|}{v}\right)\right] \qquad for\ i = 1,\ldots,4 \qquad (5)$$

where A_{RO}, A_{RE} *and* l_W are the amplitude and length of the sine waves, respectively. Time and velocity are represented by t and v, respectively. The time lag of the wheels is defined according to the contact points distances (see Figure 2) and velocity.

2.5 Track-Bridge Equations

The track-bridge element in Figure 3 is composed by the rail upper-beam and the bridge lower-beam connected by the ballast stiffness and damping elements. The formulation is based on chapter 6 of Xiaoyan Lei's book [15]

The stiffness, damping and mass matrices of the system depend on the following shape functions:

$$\{N\} = \begin{Bmatrix} U_1 \\ V_1 \\ M_1 \\ U_2 \\ V_2 \\ M_2 \end{Bmatrix} = \begin{Bmatrix} 1 - \dfrac{x}{L} \\ 1 - \dfrac{3x^2}{L^2} + \dfrac{2x^3}{L^3} \\ x - \dfrac{2x^2}{L} + \dfrac{x^3}{L^2} \\ 1 - \dfrac{x}{L} \\ \dfrac{3x^2}{L^2} - \dfrac{2x^3}{L^3} \\ -\dfrac{x^2}{L} + \dfrac{x^3}{L^2} \end{Bmatrix} \tag{6}$$

This vector can be divided into the axial degrees-of-freedom shape functions vector:

$$\{N_u\} = \begin{Bmatrix} 1 - \dfrac{x}{L} \\ 1 - \dfrac{x}{L} \end{Bmatrix} \tag{7}$$

and into the bending degrees-of-freedom shape functions vector:

$$\{N_v\} = \begin{Bmatrix} 1 - \dfrac{3x^2}{L^2} + \dfrac{2x^3}{L^3} \\ x - \dfrac{2x^2}{L} + \dfrac{x^3}{L^2} \\ \dfrac{3x^2}{L^2} - \dfrac{2x^3}{L^3} \\ -\dfrac{x^2}{L} + \dfrac{x^3}{L^2} \end{Bmatrix} \tag{8}$$

The stiffness matrix of the rail can be obtained with the equation:

$$[k_R]^e = E_R I_R \int_0^L \{N_v''\}^T \{N_v''\} dx + E_R A_R \int_0^L \{N_u'\}^T \{N_u'\} dx + k_{BL} \int_0^L \{N\}^T \{N\} dx \tag{9}$$

The mass matrix of the rail can be obtained with the equation:

$$[m_R]^e = m_R \int_0^L \{N\}^T \{N\} dx \tag{10}$$

The viscous damping matrix of the rail can be obtained with the equation:

$$[c_R]^e = [c_R] + c_{BL} \int_0^L \{N\}^T \{N\} dx \tag{11}$$

where $[c_R]^e$ is obtained using Rayleigh´s method:

$$[c_R] = a_0[m_R] + a_1[k_R] \tag{12}$$

$$\mathrm{a_0} = \xi \frac{2\omega_\mathrm{i}\omega_\mathrm{j}}{\omega_\mathrm{i}\omega_\mathrm{j}} \tag{13}$$

$$\mathrm{a_1} = \frac{2\xi}{\omega_\mathrm{i}\omega_\mathrm{j}} \tag{14}$$

where ξ represents the damping ratio and ω_i and ω_j are the first and second natural rail frequencies. Similarly, the stiffness $[k_B]^e$, mass $[m_B]^e$ and damping $[c_B]^e$ matrices can be obtained. The stiffness matrix of the prestressed concrete bridge can be obtained with the equation:

$$[k_B]^e = E_B I_B \int_0^L \{N_v"\}^T \{N_v"\}\, dx + E_B A_B \int_0^L \{N_u'\}^T \{N_u'\}\, dx + k_{BL} \int_0^L \{N\}^T \{N\} dx \tag{15}$$

The mass matrix of the prestressed concrete bridge can be obtained with the equation:

$$[m_B]^e = m_B \int_0^L \{N\}^T \{N\} dx + m_{BL} \int_0^L \{N\}^T \{N\} dx \tag{16}$$

The viscous damping matrix of the prestressed concrete bridge can be obtained with the equation:

$$[c_B]^e = [c_B] + c_{BL} \int_0^L \{N\}^T \{N\}\, dx \tag{17}$$

where $[c_B]$ is obtained using Rayleigh´s method:

$$[c_B] = a_0[m_B] + a_1[k_B] \tag{18}$$

The stiffness $[k_{BL}]^e$ and damping matrices of the ballast $[c_{BL}]^e$ are computed in the following way, respectively:

$$[k_{BL}]^e = k_{BL}\int_0^L \{N\}^T\{N\}dx \tag{19}$$

$$[c_{BL}]^e = c_{BL}\int_0^L \{N\}^T\{N\}dx \tag{20}$$

Equation (19) and equation (20) serve to interpolate the discrete value k_{BL} and c_{BL} in the finite elements of the bridge and the rail.

The result of $\int_0^L \{N\}^T\{N\}\,dx$ is:

$$\frac{L}{420}\begin{bmatrix} 140 & 0 & 0 & 70 & 0 & 0 \\ 0 & 156 & 22L & 0 & 54 & -13L \\ 0 & 22L & 4L^2 & 0 & 13L & -3L^2 \\ 70 & 0 & 0 & 140 & 0 & 0 \\ 0 & 54 & 13L & 0 & 156 & -22L \\ 0 & -13L & -3L^2 & 0 & -22L & 4L^2 \end{bmatrix} \tag{21}$$

The result of $EI\int_0^L \{N_v"\}^T\{N_v"\}dx + EA\int_0^L \{N_u'\}^T\{N_u'\}dx$ is:

$$\begin{bmatrix} \frac{EA}{L} & 0 & 0 & \frac{EA}{L} & 0 & 0 \\ 0 & \frac{12EI}{L^3} & \frac{6EI}{L^2} & 0 & -\frac{12EI}{L^3} & \frac{6EI}{L^2} \\ 0 & \frac{6EI}{L^2} & \frac{4EI}{L} & 0 & -\frac{6EI}{L^2} & -\frac{2EI}{L} \\ \frac{EA}{L} & 0 & 0 & \frac{EA}{L} & 0 & 0 \\ 0 & -\frac{12EI}{L^3} & -\frac{6EI}{L^2} & 0 & \frac{12EI}{L^3} & -\frac{6EI}{L^2} \\ 0 & \frac{6EI}{L^2} & \frac{2EI}{L} & 0 & -\frac{6EI}{L^2} & \frac{4EI}{L} \end{bmatrix} \tag{22}$$

The interaction of the vehicle model is uncoupled, that is, the vehicle's force is calculated in order to obtain the force applied on the structure. After that, the bridge structure is calculated considering the influence of the ballast and the rail.

The equation of motion of the track- bridge interaction is given by:

$$[M]\{\ddot{U}(t)\} + [C]\{\dot{U}(t)\} + [K]\{U(t)\} = \{F_{R_i}(t)\} \tag{23}$$

$$[M] = [m_R] + [m_B] \tag{24}$$

$$[C] = [c_R] + [c_B] - [c_{BL}] \tag{25}$$

$$[K] = [k_R] + [k_B] - [k_{BL}] \tag{26}$$

Where:

- k_{BL} is the discrete value of ballast stiffness;
- m_{BL} is the discrete value of ballast mass;
- c_{BL} is the discrete value of ballast damping;
- A_R, E_R, I_R are the rail area, Young´s modulus and moment of inertia, respectively;
- A_B, E_B, I_B are the bridge area, Young´s modulus and moment of inertia, respectively;

$\{F_{R_i}(t)\}$ is obtained in equation (3).

3 PROGRAM DESCRIPTION

The program is described briefly in Figure 5.

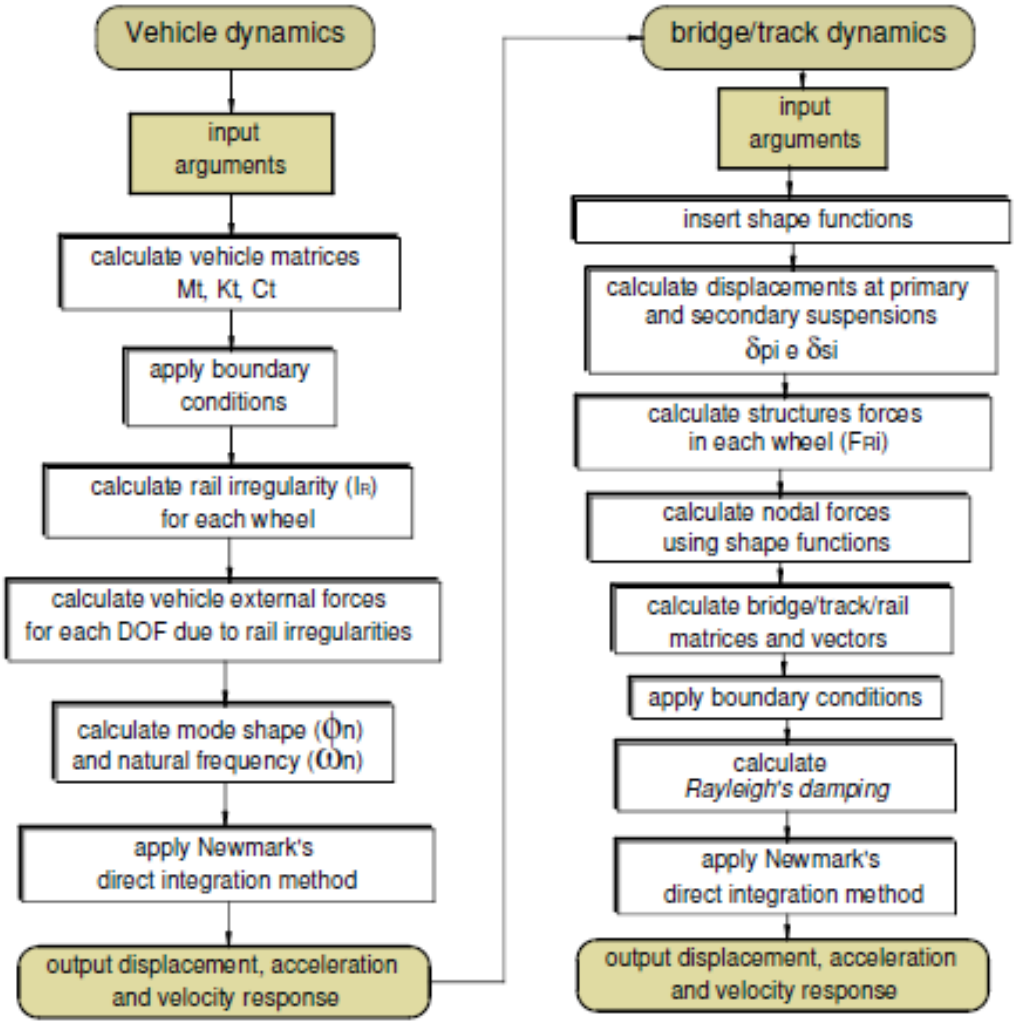

Figure 5: Flow chart illustrating vehicle-track-bridge interaction

4 NUMERICAL EXAMPLE

This section presents the dynamic response of the bridge as well as the bridge, vehicle and track properties considered in this study.

4.1 Vehicle analysis

Table 1 Dynamic properties of rigid body

Rigid bodies	Parameters	Symbols	Values	Units
Car body	mass	m_{CB}	44420	kg
	Moment of inertia in X	I_{XCB}	1816726.269	kg/m²
	Moment of inertia in Y	I_{YCB}	57925.731	kg/m²
Front bogie	mass	m_{FB}	14000	kg
	Moment of inertia in X	I_{XFB}	26469.468	kg/m²
	Moment of inertia in Y	I_{YFB}	11150.037	kg/m²
Rear bogie	mass	m_{FB}	14000	kg
	Moment of inertia in X	I_{XRB}	26469.468	kg/m²
	Moment of inertia in Y	I_{YRB}	11150.037	kg/m²
Wheels	mass	m_W	750	kg

Table 2 Dynamic properties of the suspensions system

Itens	Symbols	Values	Units
Primary suspension	K_P	1606.09	kN/m
	C_P	31.152	kNs/m
Secondary suspension	K_S	429.51	kN/m
	C_S	17.089	kNs/m

Table 3 Geometric distances

Distances	Symbols	Values	Units
longitudinal distance of center of bogies	2a	15	m
longitudinal distance of center of wheels	2b	3	m
cross distance of center of wheels	2c	1.6	m

Table 4 Irregularities properties

Itens	Symbols	Values	Units
vehicle velocity	v	50	km/h
amplitude of the sine waves on the rail *RO*	A_{RO}	0.01	m
amplitude of the sine waves on the rail *RE*	A_{RE}	0.01	m
lenght of the sine waves	l_W	1.0	m

4.2 Bridge analysis

Table 5 Bridge Properties E_{cs} = 25187 MPa (f_{ck} = 28 MPa)

Element	Length	Area	Moment of Inertia	Mass
	m	m²	m^4	kg/m³
1-3/28-30/31-33/58-60	1.0	2.822	2.948	2500
4-27/34/57	1.0	1.911	2.563	2500
61/63	2.1	1.1007	0.388	2500
62	2.1	1.1007	0.388	2500

Where:

- Ecs is the Young´s modulus of the bridge concrete
- fck is the bridge concrete resistance in 28 days

The bridge total length is 30.0 m and the considered damping is 1.0 % when considering ballast influence and 2.5 % when not considering ballast influence.

4.3 Ballast analysis

Table 6 Ballast properties

Stiffness (k_{BL})		Damping (C_{BL})	
Vertical	Horizontal	Vertical	Horizontal
$6x10^4$ kN/m²	$6x10^4$ kN/m²	50 kNs/m²	50 kNs/m²

4.4 Rail analysis

Table 7 Rail properties

Geometric properties of the rails	Symbols	Values	Units
cross sectional área	A	8.63E-03	m²
moment of inertia in Z	I_Z	3.95E-05	m^4

The rail damping considered is 0.5%.

5 RESULTS

The dynamic response analysis of the bridge is performed on the mid span, considering the vehicle velocity of 50 km/h. Figure 6 shows the influence of the ballast and of track irregularities on the vertical displacement of the mid span during the passage of the vehicle.

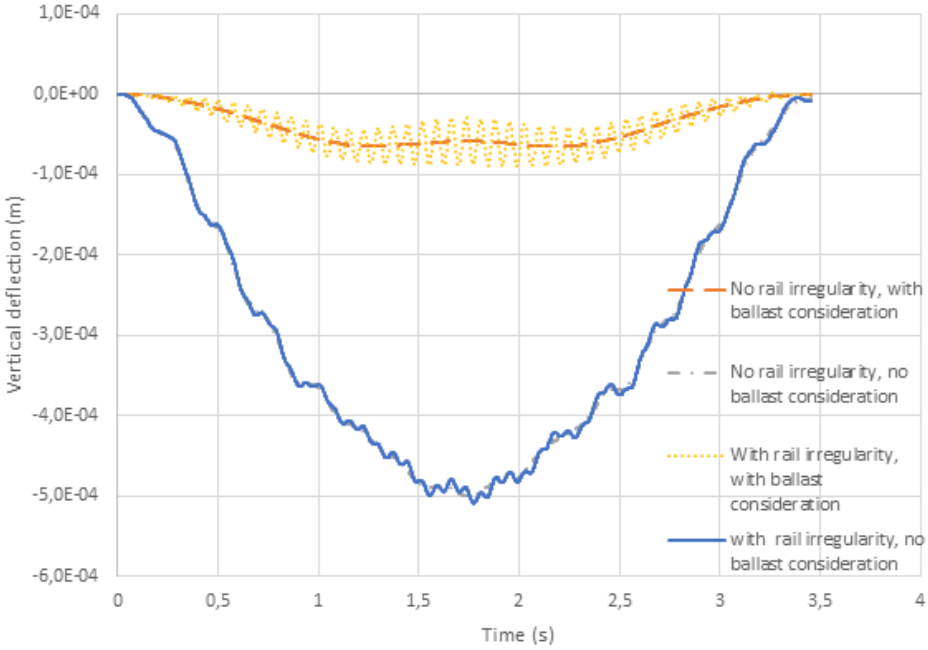

Figure 6: Track irregularities and ballast influence on the vertical displacement

As it can be observed from these results, when considering the influence of the ballast on the calculation the displacement on the bridge reduces.

In this case, the ballast stiffness k_{BL} considered is 6xE+04 kN/m² and the ballast damping c_{BL} considered is 50 kN.s/m², which are average of the values in references [2]-[13]. The maximum mid span deflection is 9.10xE-04 m (yellow dotted line) and is obtained at 2.21 seconds, considering rail irregularities. With no rail irregularities the maximum mid span deflection reduces to 6.54xE-04 m at 2.62 seconds (orange dashed line), which represents a reduction of 27%.

When not considering the ballast influence, the maximum mid span deflection, which occurs at 1.75 second, is 5.1xE-04 m (gray axis line). With no track irregularities consideration, the maximum mid span deflection reduces to 5.0xE-04 m at 1.75 second (orange dashed line), which represents a reduction of 1%.

The mid span deflection has more variation when considering track irregularities and ballast stiffness as it can be observed at the yellow dotted line.

The deflection decreases around 82% - 87% when considering ballast stiffness.

These percentages are obtained dividing the maximum mid span deflection with ballast consideration by the mid span deflection without ballast consideration.

Figure 7 shows the influence of the ballast stiffness on the vertical displacement. The ballast stiffness varies from 1.0xE+03 kN/m² to 1.0xE+05 kN/m², and the effect of this variation is depicted in the figure.

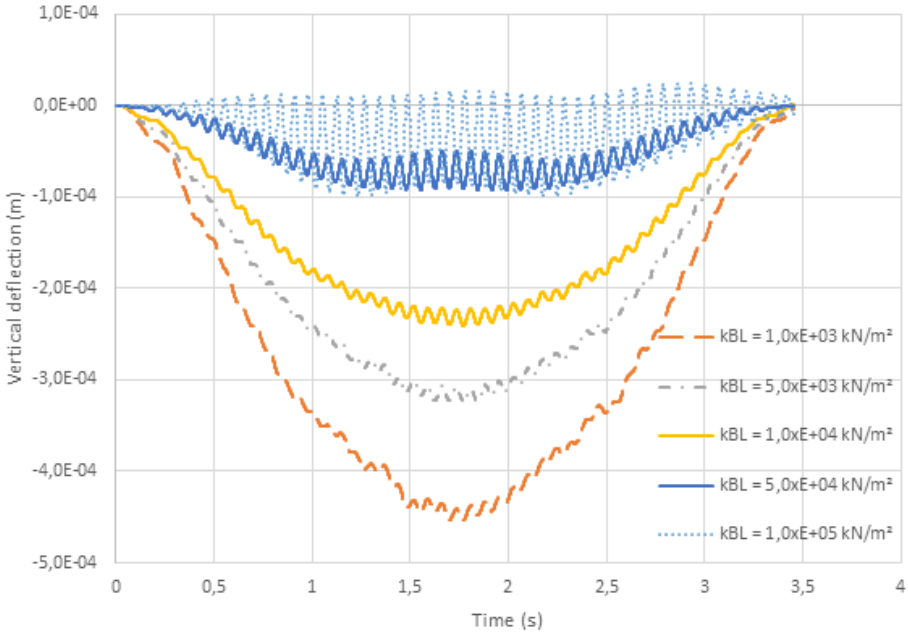

Figure 7: Ballast stiffness influence on the vertical displacement

The figure compares the influence on the mid span vertical displacement adopting five different ballast stiffness values from other references [2]-[13] .

As it can be observed, the higher is the ballast stiffness, the lower is the mid span deflection and the higher is the track irregularity influence (higher amplitude).

Table 8 Ballast stiffness influence

Ballast stiffness (kN/m²)	Ballast stiffness reduction*	Line	Maximum displacement (m)	Time (s)	Displacement reduction*
1.0xE+03	99%		4.54x-04	1.77	0.00%
5.0xE+03	95%		3.25x-04	1.77	28.51%
1.0xE+04	90%		2.40x-04	1.77	47.03%
5.0xE+04	50%		9.25x-05	1.99	79.63%
1.0xE+05	0%		9.91x-05	1.23	78.16%

*The reductions are obtained comparing the values on the table with the maximum value of the column.

Figure 8 shows the influence of the ballast damping on the vertical displacement. The ballast damping values have been obtained from references [2]-[13] and their values are 0 kN.s/m², 25 kN.s/m², 50 kN.s/m², and 80 kN.s/m². No significant effect is observed which leads to the understanding that ballast damping has not great influence on the bridge´s displacement.

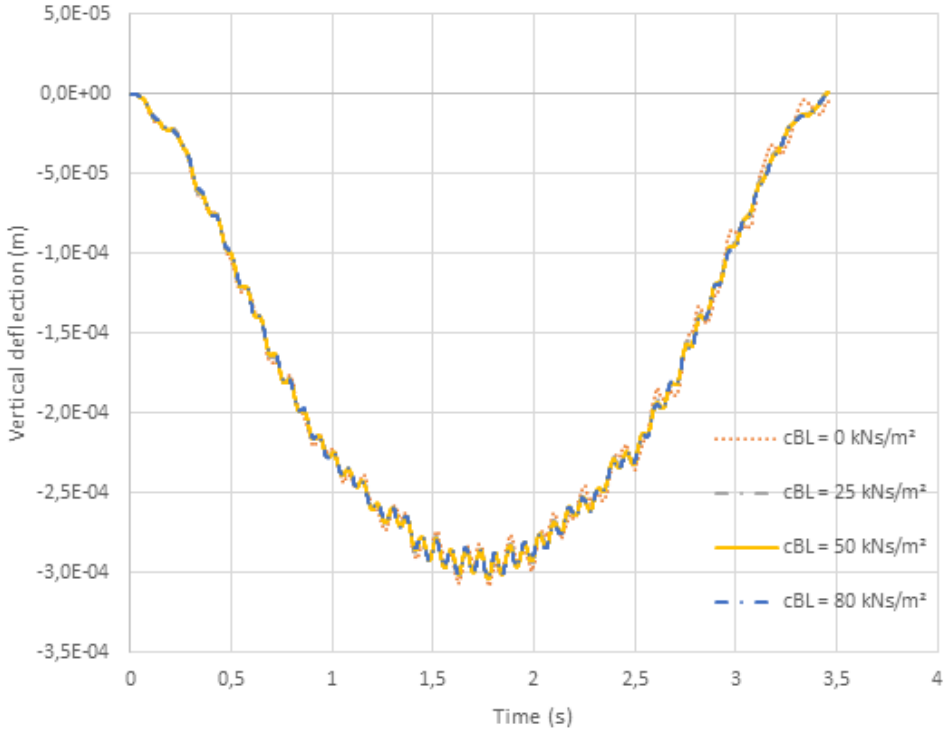

Figure 8: Ballast damping influence on the vertical displacement

6 CONCLUSION

This work aims to analyze the dynamic responses of railway track and bridge under moving loads. The dynamic behavior of the railway track-bridge model is studied integrating the rail, ballast, and bridge. The rails are modeled as elastic Euler-Bernoulli upper beams and the bridge as an Euler-Bernoulli lower beam discretized by finite elements. The sleepers and ballast are modeled using Winkler foundation for translation.

The vehicle is a 9 degree-of-freedom model composed of an association of rigid bodies connected via suspension systems. The dynamic responses of the vehicle are obtained due to the speed and tracks irregularities, which are considered as harmonic sinusoidal functions. After that, the vehicle wheel forces are applied on the railway track-bridge model. The vector of the external forces is composed by arranging vehicle mass and inertial forces.

The equations of motion of both systems are integrated using the Newmark's method.

The displacements at mid span have been analyzed and compared. The ballast stiffness and damping values considered have been taken from other works [2]-[13], and results due to value variations are also compared here.

Vertical displacements at the mid span reduce when ballast effects are considered. The first verification uses an average value for ballast stiffness and damping and compares it with a no-ballast situation. The deflection reduction varied from 82% to 87%. It is also observed that track irregularities have higher amplitudes when ballast is stiffer.

The second verification compares the effect of different ballast stiffness values. It is observed that deflection reduces considerably as well as the influence of track irregularities amplitude increases as ballast stiffness increases.

Finally, different values of damping are compared but no significant results are obtained. It appears that ballast damping may not be important in the bridge dynamic behavior. However, further investigations would have to be conducted to allow for a sound conclusion.

From this research, we can conclude that ballast stiffness has great influence on the results.

Track irregularities also have an important role on dynamic analysis. For more realistic responses, the authors shall consider random track irregularities instead of harmonic track irregularities.

7 ACKNOWLEDGEMENTS

The first author would like to acknowledge the support provided by Universidade Tecnológica Federal do Paraná and CAPES.

REFERENCES

[1] L. Fryba, (1996), Dynamics of railway bridges, Thomas Telford, London.

[2] Z. Cai, G. P. Raymond and J. O. Igwemezie, (1994), Contact loads from vertical dynamic wheel/rail and track interaction, Fourth International Conference on Contact Mechanics and Wear of Wheel/Rail Systems, Vancouver.

[3] Y. S. Cheng, F. T. K Au and Y. K Cheng, (2001), Vibration of railway bridges under a moving train by using bridge-track-vehicle element, Engineering Structures, Great Britain, v. 23, p. 1597 – 1606.

[4] Walber da Luz Correa, (2008), Controle de vibrações induzidas pela interação dinâmica entre trens-trilho-dormente-estrutura de aço de pontes ferroviária. Rio de Janeiro (Tese). Universidade Federal do Rio de Janeiro, 2008.

[5] T. Dahlberg, (2006), Handbook of Railway Vehicle Dynamics, Track Issues, Taylor & Francis Group, LLC.

[6] G. Di Mino and C. M. Di Liberto, (2007), A model of dynamic interaction between a train vehicle and a rail track, 4th International SIIV Congress – Palermo (Italy), 12-14 September.

[7] Carlos Alberto B. Guimarães, (1999), Análise das solicitações dinâmicas na via férrea através da simulação da interação entre o veículo e a via. Tese de doutorado, Universidade Estadual de Campinas, Unicamp, Campinas.

[8] Vu Hieu Nguyen, (2002), Comportement dynamique de structures non-linéaires soumises à des charges mobiles, L'ecola Nationale des Ponts e Chaussees, França.

[9] T. Rauert, H. Bigelow, B. Hoffmeister and M. Feldmann, (2012), On the prediction of the interaction, effect caused by continuous ballast on filler beam railway bridges by experimentally supported numerical studies. Engineering Structures 32, 3981–3988.

[10] Constança Rigueiro et al, (2010) Influence of ballast models in the dynamic response of railway viaducts. Department of Civil Engineer EST, Institute Polytechnic of Castelo Branco. Journal of Sound and Vibration 329, 3030–3040.

[11] P. Ruge and C Birk, Longitudinal forces in continuously welded rails on bridgedecks due to nonlinear track-bridge interaction. Computers & Structures, n. 85, p. 458-475, 2007.

[12] P. Ruge, D. R. Widarda, G. Schmälzlin and G. Bagayoko, (2009), Longitudinal track-bridge interaction due to sudden change of coupling interface. Computers and Structures, 87, p. 47-58.

[13] Y. B. Yang, J. D. Yau and Y. S. Wu, (2004), Vehicle-Bridge Interaction Dynamics: With application to High-Speed Railways. Chapter 9, World Scientific Publishing Co. Pte. Ltd., Singapore.

[14] F. L. M. Beghetto, (2006), Efeitos dinâmicos em modelo de veículo e ponte ferroviária diante da variação de velocidade e irregularidades verticais da via. Dissertação, Pontifícia Universidade Católica do Paraná, Curitiba.

[15] Xiaoyan Lei, (2016), High Speed Railway Track Dynamics: Models, Algorithms and Applications. Chapter 6, Science Press, Beijing.

RESPONSIBILITY NOTICE

The authors are the only responsible for the printed material included in this paper.